THE JOURNAL OF PHYSICAL CHEMISTRY A

 VOLUME 108, NUMBER 13, APRIL 1, 2004

ARTICLES

Picosecond Relaxation of ^{3}MLCT Excited States of $[Re(Etpy)(CO)_3(dmb)]^+$ and $[Re(Cl)(CO)_3(bpy)]$ as Revealed by Time-Resolved Resonance Raman, UV−vis, and IR Absorption Spectroscopy

Davina J. Liard,[†] Michael Busby,[†] Pavel Matousek,[‡] Michael Towrie,[‡] and Antonín Vlček, Jr.*,[†]

Department of Chemistry and Centre for Materials Research, Queen Mary, University of London, Mile End Road, London E1 4NS, United Kingdom, and Central Laser Facility, CCLRC Rutherford Appleton Laboratory, Chilton, Didcot, Oxfordshire OX11 0QX, United Kingdom

Received: September 3, 2003; In Final Form: December 11, 2003

Picosecond dynamics of Re → polypyridine ^{3}MLCT excited states of $[Re(Etpy)(CO)_3(dmb)]^+$ and $[Re(Cl)(CO)_3(bpy)]$ were investigated by time-resolved UV−vis, resonance Raman, and IR spectroscopy. Raman bands due to $NN^{\bullet-}$ intraligand vibrations of the excited molecules increase with time during the first 15−20 ps after excitation. The time constant of 6 ± 2 ps was estimated for the increase of areas of excited-state Raman bands of $[Re(Etpy)(CO)_3(dmb)]^+$. The growth of Raman bands is accompanied by an increase of the near-UV transient absorption band at 375 nm, which corresponds to a $\pi\pi^*$ transition of the $dmb^{\bullet-}$ ligand of the ^{3}MLCT excited state $[Re^{II}(Etpy)(CO)_3(dmb^{\bullet-})]^+$. These effects are attributed to structural reorganization during vibrational cooling, during which the electronic dipole moment and/or vibrational overlap integrals increase. IR bands due to CO stretching vibrations and some of the Raman bands undergo dynamical upward shift and narrowing, that occur with time constants between 1 and 11 ps, manifesting cooling of anharmonically coupled low-frequency vibrational modes. These observations demonstrate that relaxation dynamics of ^{3}MLCT excited states of metal-polypyridine complexes extend into the picosecond time domain. It follows that many important ultrafast photochemical processes of metal polypyridine complexes, such as electron injection into semiconductors, actually occur from unequilibrated, vibrationally excited states.

Introduction

Polypyridine complexes of d^6 metals (Ru^{II}, Os^{II}, Re^{I}) are important photosensitizers[1−4] of energy- and electron-transfer reactions with possible applications in light energy conversion and as components of molecular electronic or photonic devices. Many of the processes involved are ultrafast, occurring on a femtosecond−picosecond time scale. An important example is photosensitization of semiconductor electrodes in solar cells, which starts with femtosecond electron injection from a metal to ligand charge transfer (MLCT) excited state of a polypyridine complex.[5−11] Intramolecular photochemical reduction or oxidation of the axial ligand L is another important class of ultrafast photochemical reactions pertinent especially to $[Re^{I}(L)(CO)_3(NN)]^{n+}$ (NN = polypyridine) complexes.[3,12−18] These reactions result in either formation of a charge-separated state[3,12−14,16,17,19−22] or fragmentation[15,23−25] of the ligand L. Understanding and utilizing such ultrafast reactions require to understand the early relaxation processes of MLCT excited states of M(polypyridine) chromophores, since they can affect and/or compete with the

[†] University of London.
[‡] CCLRC Rutherford Appleton Laboratory.

10.1021/jp0366320 CCC: $27.50
Published on Web 03/09/2004

productive electron- or energy-transfer reactions. The rate and mechanism of localization of the excited electron is the most important question for Ru(II) or Os(II) complexes of the type $[M(NN)_3]^{2+}$ or $[M(NN)_2L_2]^{2+}$. Recent studies have shown that this is a convoluted process of electron-density redistribution, intersystem crossing, and intramolecular vibrational energy redistribution that is essentially completed in the first ~300 fs after excitation.[7,26−28] However, slower relaxation steps and electron hopping between polypyridine ligands can extend into the picosecond time domain.[29−33] Electron localization is not an issue for $[Re(L)(CO)_3(NN)]^{n+}$, which contains only a single Re(NN) chromophore.[2,3,34−38] Morever, they are photostable with respect to ligand dissociation. These compounds are thus well amenable to investigations of structural changes and early relaxation dynamics that follow the large electron-density redistribution caused by optical Re → NN MLCT excitation.

Herein, we have concentrated on a cationic complex $[Re(Etpy)(CO)_3(dmb)]^+$ (dmb = 4,4′-dimethyl-2,2′-bipyridine, Etpy = 4-ethylpyridine) and investigated its early excited-state dynamics by picosecond time-resolved Raman (TR^3) and IR absorption (TRIR) spectroscopy, which reveal the time-dependent structural changes of the dmb and $Re(CO)_3$ moieties, respectively. Unexpectedly, we have observed a delayed appearance of Raman bands in the TR^3 spectra. Interpretation of this effect is aided by time-resolved UV−vis absorption spectroscopy, whose femto−picosecond dynamics was, for the first time, investigated in the near-UV spectral region. For comparison, we have carried out similar experiments on the analogous complex $[Re(Cl)(CO)_3(bpy)]$.

Experimental Section

$[Re(Etpy)(CO)_3(dmb)]PF_6$ and $[Re(Etpy)(CO)_3(bpy)]PF_6$ were synthesized and characterized as described previously.[13,39] Literature procedures[36,40] were followed to prepare $[Re(Cl)(CO)_3(bpy)]$, $[Re(Cl)(CO)_3(phen)]$, and $[Re(Cl)(CO)_3(^i\text{Pr-DAB})]$. Solutions for spectroscopic measurements were prepared in acetonitrile (Aldrich, spectrophotometric grade).

Time-resolved visible, IR, Kerr-gate resonance Raman, and Kerr-gate emission used the equipment and procedures described in detail previously.[14,41−46] In short, the sample solution was excited (pumped) at 400 nm, using frequency-doubled pulses from a Ti:sapphire laser of ~200 fs duration (fwhm) in the case of time-resolved IR absorption spectroscopy, while pulses of 1−2 ps duration were used for Raman and emission studies. TRIR spectra were probed with IR (~200 fs) pulses obtained by difference-frequency generation. IR probe pulses cover a spectral range 150−200 cm^{-1} wide. Kerr-gate TR^3 spectra were measured using 1−2 ps, 400 nm pump pulses and probed at 400 nm using frequency-doubled Ti:sapphire laser pulses. In some experiments, we used pump or probe pulses at 350 nm which were generated by mixing the 622 nm OPA output with the 800 nm Ti:sapphire fundamental. The pump and probe pulse energies of 4.4 and 5.6 μJ, respectively, were used. (A larger probe than pump pulse energy was needed because of the weakness of the excited-state signal.) The laser beams were focused to an area of a ~150 μm diameter. The Kerr gate was opened for ca. 4 ps coincidentally with the probe pulse, using a fraction of the 800 nm output of the Ti:sapphire laser. In this way, all the long-lived emission is removed from the Raman signal. TR^3 spectra were corrected for the Raman signal due to the solvent and the ground state by subtracting the spectra obtained at negative time delays (−50, −20 ps) and by subtracting any weak residual emission that passed through the Kerr gate. Measurements of antistokes TR^3 spectra was attempted using pumping and probing at 400 nm, both pulses having the same energy of ~8 μJ. Strong emission prevented us from measuring the ground-state preresonance Raman spectrum of $[Re(Etpy)(CO)_3(dmb)]^+$ by a conventional Raman spectrometer using cw lasers. Instead, this spectrum was obtained using the Kerr-gate TR^3 instrument with the pump-beam blocked. The ground-state Raman scattering is then generated by the probe beam while interfering emission is removed by the Kerr gate.

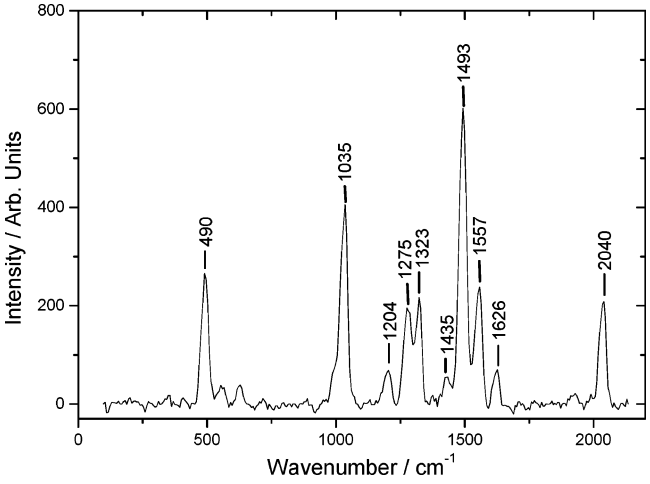

Figure 1. Preresonance Raman spectrum of $[Re(Etpy)(CO)_3(dmb)]^+$ in CH_3CN measured with 400 nm laser pulse (1−2 ps) excitation. Interfering emission was rejected using 4 ps optical Kerr gate.

Time-resolved UV−vis absorption spectra were measured using the experimental setup available at the Institute of Molecular Chemistry, University of Amsterdam, that is described in ref 47. A ~130 fs, 395 nm pump pulse was generated by frequency doubling of the Ti:sapphire laser output. White-light continuum probe pulses in the near UV spectral region were generated by focusing the 800 nm fundamental on a rotating BaF_2 plate.

All Raman spectra were measured from sample solutions flowed as a 500 μm diameter open jet. A 0.5 mm flow-through rastering CaF_2 cell was used to obtain TRIR spectra. The pump and infrared probe beams are focused to less than 200 μm diameter. A 2 mm fused silica cell was used to measure TR UV−vis spectra.

Results

Electronic Absorption, Resonance Raman, and Emission Spectra. $[Re(Etpy)(CO)_3(dmb)]^+$ shows broad absorption at ~339 nm (5700 M^{-1} cm^{-1}) in CH_3CN, which shifts to 344 and 354 nm in MeOH and $ClCH_2CH_2Cl$, respectively. This small solvatochromism suggests a Re → dmb character of the transition responsible. This assignment is confirmed by the preresonance Raman spectrum of $[Re(Etpy)(CO)_3(dmb)]^+$ measured using 400 nm excitation, Figure 1, which shows resonance-enhanced Raman bands corresponding to vibrations of the dmb ligand,[48] the in-phase A′(1) ν(CO) vibration, and coupled skeletal stretching and deformation modes. This resonance Raman pattern manifests displacements of skeletal, CO and intra-dmb normal modes upon MLCT excitation. It is indicative[49] of a localized Re → dmb MLCT character of the resonant transition.

Time-resolved Kerr-gate emission spectra of $[Re(Etpy)(CO)_3(dmb)]^+$ in CH_3CN show a broad band which shifts from ca. 530 to 540 nm between 10 and 40 ps after excitation, due to relaxation processes. No changes in emission intensity were seen

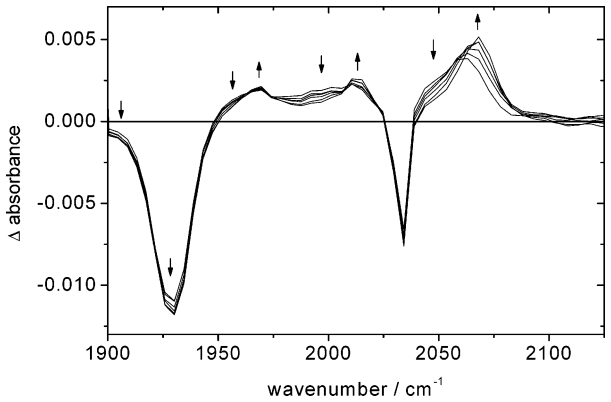

Figure 2. Difference TRIR spectra of [Re(Etpy)(CO)$_3$(dmb)]$^+$ in CH_3CN. Spectra measured at 1, 2, 3, 6, 11, and 100 ps after 400 nm; ~200 fs laser pulse excitation are shown. Spectra evolve in the directions of the arrows. Negative peaks correspond to depleted ground-state population. Positive bands are due to the photogenerated transient. Experimental points are ca. 4 cm^{-1} apart. Raman band assignment:[48,50−53] 2040 (0.37) A′(1) ν(CO); 1626 cm^{-1} (0.14) ν(CC$_{Me}$)/ν(CC)$_{ir}$/ν(CN); 1557 cm^{-1} (0.42); ν(CC)/ν(CN)/δ(CCH); 1493 cm^{-1} (1); δ(CCH)/ν(CC)/ν(CC)$_{ir}$/ν(CN); 1435 cm^{-1} (0.13) δ(CCH)/ν(CC)/ν(CN); 1323 cm^{-1} (0.38) δ(CCH)/ν(CC)$_{ir}$; 1275 cm^{-1} (0.35); ν(CC)/ν(CN); 1204 cm^{-1} (0.14); δ(CCH); 1035 cm^{-1} (0.68); δ(CCH)/ν(CC)/δ(CCC); 490 cm^{-1} (0.46); ν(ReN)/ν(ReC)/δ(NReN). (Numbers in parentheses are relative band intensities with respect to the 1493 cm^{-1} band, ir = inter-ring.)

at longer time delays up to 1 ns, in agreement with the long ^{3}MLCT excited-state lifetime (510 ± 20 in 1,2-dichloroethane, ref 54). An identical band is seen in the steady-state emission spectrum.[55]

Time-Resolved IR Spectroscopy. Shown in Figure 2 is the picosecond TRIR spectrum of [Re(Etpy)(CO)$_3$(dmb)]$^+$ in CH_3CN. Spectra measured at long time delays after excitation (>50 ps) correspond well to the excited-state spectrum that was obtained on a ~100 ns time scale using the step-scan FTIR technique.[55] The ground- and excited-state ν(CO) spectral patterns are quite different. The ground-state spectrum shows a sharp band due to the A′(1) in-phase ν(CO) vibration at 2034 cm^{-1} and a broad band at 1930 cm^{-1} due to an unresolved out-of-phase A′(2) and asymmetric A″ vibrations. This spectral pattern is characteristic of a pseudo-C_{3v} local symmetry of the Re(CO)$_3$ fragment, which reflects similar bonding properties of the dmb and Etpy ligands toward Re. In contrast, the excited-state spectrum shows three ν(CO) bands. The A″ and A′(2) bands are well separated at 1970 and 2013 cm^{-1}, respectively. The A′(1) vibration occurs at 2068 cm^{-1}. (The peak wavenumbers were measured at time delays of 100 ps and longer. The assignment is based on ref 55)

The large positive shifts of all ν(CO) bands upon excitation (+34 cm^{-1} for the A′(1) band, ca. +50 cm^{-1} on the average) testify to the Re → dmb MLCT character of the excited state. It is caused by a decrease of Re → CO π back-donation and increase of OC → Re σ donation.[55] The magnitude of this shift is comparable to those found for typical MLCT excited states in analogous complexes [Re(Cl)(CO)$_3$(4,4′-bipyridine)$_2$] and [Re(Cl)(CO)$_3$(bpy)], 54 and 55 cm^{-1}, respectively.[56,57] It is, however, smaller than that found[55] for [Re(Etpy)(CO)$_3$(4,4′-(COOEt)$_2$-bpy)]$^+$ (63 cm^{-1}), indicating that the Re/bpy charge separation is larger if the bpy ligand bears electron-accepting substituents. The band shape of all IR bands investigated herein is Lorentzian, as expected.[58] The integrated IR band areas are time-independent ower the whole time-range investigated.

It can be seen from Figure 2 that the shift of ν(CO) IR bands from their ground-state positions consists of two parts: an "instantaneous shift" that is completed within the instrument time resolution (<1 ps) and following picosecond upward shift, whereby the ν(CO) bands move to higher wavenumbers while their bandwidths decrease. Band-narrowing seems to be the largest for the middle A′(2) band. These dynamical effects can best be analyzed for the highest A′(1) band. Its maximum shifts by +11.4 ± 0.8 cm^{-1} with a biexponential dynamics: 1.3 ± 0.2 ps (74%) and 11.6 ± 2.1 ps (26%).[59] The bandwidth decreases exponentially by ca. 24% with a time constant of 9.8 ± 1.8 ps. In principle, picosecond positive band shifts originate in vibrational relaxation and solvation, while narrowing reflects vibrational relaxation only.[33] Dynamical solvation effects will not contribute in CH_3CN, whose relaxation time (260 fs)[60] is faster than the experimental time-resolution. Hence, both band shift and narrowing observed herein are expected to reflect only the vibrational relaxation. Indeed, the band-narrowing and band-shift dynamics are identical, within the experimental accuracy. The same behavior was observed for [Re(Cl)(CO)$_3$(4,4′−R$_2$-bpy)] (R = COOH, COOEt) in fast-relaxing DMF or at ZrO_2 surfaces, where solvation is absent.[33]

Time-Resolved Raman Spectroscopy and UV−vis Absorption. Nanosecond transient Raman spectra of ^{3}MLCT excited states of [Re(Etpy)(CO)$_3$(bpy)]$^+$, [Re(Cl)(CO)$_3$(bpy)], and Ru^{II} or Os^{II} polypyridine complexes usually show reasonably intense peaks due to the dmb$^{\bullet-}$ or bpy$^{\bullet-}$ chromophore when excited by high-intensity nanosecond UV laser, usually at 354.7 or 368.9 nm.[20,50,61,62] In contrast, we have observed only very weak Raman signals for [Re(Etpy)(CO)$_3$(dmb)]$^+$ and [Re(Cl)(CO)$_3$(bpy)] in the picosecond time domain, regardless of the Raman probe wavelength, 400 or 350 nm. This difference in transient Raman band intensities upon pico- and nanosecond excitation is due to the much larger figure of merit possessed by a nanosecond system stemming from substantially higher available pump and probe pulse energies. No picosecond Raman signal was observed for [Re(Cl)(CO)$_3$(phen)], [Re(Cl)(CO)$_3$(^{i}Pr-DAB)], and [Re(Etpy)(CO)$_3$(^{i}Pr-DAB)]$^+$, due to the lack of any strong excited-state absorption in the near-UV spectral region, which we have demonstrated independently by time-resolved UV−vis absorption spectroscopy.

Figure 3 shows the picosecond time-resolved resonance Raman (TR^3) spectrum of [Re(Etpy)(CO)$_3$(dmb)]$^+$ measured at selected time delays after 400 nm excitation. The TR^3 spectrum obtained at 100 ps shows most of the bands observed[48] in the nanosecond transient resonance Raman spectrum of the ^{3}MLCT excited state of [Ru(dmb)$_3$]$^{2+}$. This observation supports the assignment of the TR^3 bands of [Re(Etpy)(CO)$_3$(dmb)]$^+$ to vibrations of the dmb$^{\bullet-}$ ligand present in the Re → dmb ^{3}MLCT excited state. However, the overall intensity pattern of the excited-state Raman spectra of the Ru and Re complex is somewhat different. Notably, the most intense band in the TR^3 spectrum of [Re(Etpy)(CO)$_3$(dmb)]$^+$ is that at ~1500 cm^{-1} (probably a closely spaced doublet), while only a weak doublet at 1492−1507 cm^{-1} occurs in the [Ru(dmb)$_3$]$^{2+}$ spectrum. The intense doublet band at 1552−1571 cm^{-1} of [Ru(dmb)$_3$]$^{2+}$ is manifested only as a weak shoulder at ~1567 cm^{-1} for [Re(Etpy)(CO)$_3$(dmb)]$^+$. These differences are caused by different Raman probe wavelengths (400 nm vs. 369.9 nm for Ru) and by differences in the chromophore structure.

All the TR^3 bands show an unusual rise dynamics, Figures 3 and 4. They are barely apparent at 1 ps but rise in prominence over the next ca. 20 ps. This is in contrast to the ground-state resonance Raman signal "bleaches" that undergo substantially faster onset determined only by the pump and probe cross correlation (~3 ps). To analyze the rise dynamics, the TR^3

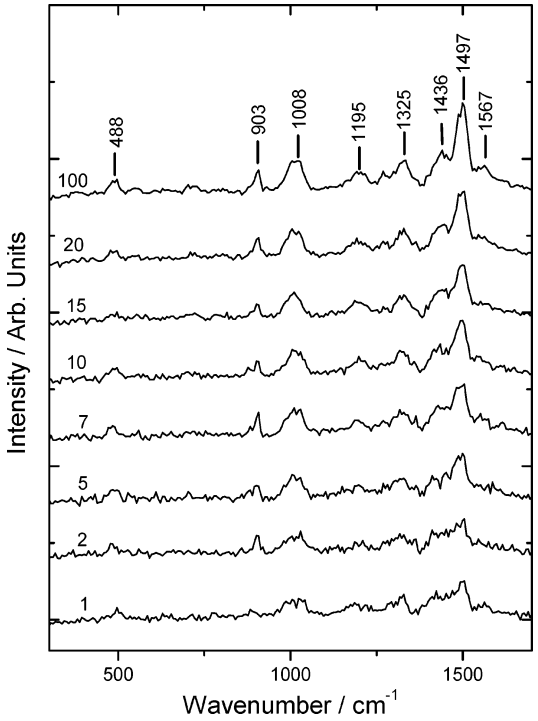

Figure 3. Picosecond time-resolved resonance Raman spectra of [Re(Etpy)$(CO)_3$(dmb)]$^+$ in CH_3CN measured at 1, 2, 5, 7, 10, 15, 20, and 100 ps after excitation with 400 nm, 1−2 ps laser pulses and probed with delayed 400 nm, 1−2 ps laser pulses. The long-lived emission was rejected using a 4 ps Kerr gate. The ground-state Raman bands of the solute and solvent were subtracted. A leakage of the pump-induced Raman signal passing through the unclosed Kerr gate at early time delays (from −5 to +5 ps) was also subtracted (this signal was separately measured in a pump-only experiment).

spectra were fitted to a sum of Lorentzian peaks to give time-dependent integrated areas, positions and widths of individual Raman peaks. The band areas increase exponentially, with time constant estimated as 6 ps, while the bandwidths decrease at a similar time scale; see Figure 4. Simultaneously, the 1497 and 1325 cm^{-1} peaks show exponential upward shifts by $+15 \pm 4$ cm^{-1}, with time-constants estimated as 10 ± 4 and 9 ± 4 ps, respectively. No reliable time dependences were obtained for positions of the other TR^3 bands. The growth and narrowing occur for all bands in the TR^3 spectra, regardless of the relative polarization of the pump and probe laser beams; parallel or perpendicular. It was also observed in the spectra measured using combinations of pump and probe wavelengths of 400 and 350 nm or 350 and 400 nm. Quantitative analysis of the rise dynamics was prevented by weakness of Raman signals in these spectra.

The dynamical upward shift of TR^3 bands is caused by cooling of anharmonically coupled low-frequency vibrations, as was discussed above for IR ν(CO) bands. Band-narrowing originates in faster collisional dephasing when the molecule and its immediate surroundings are vibrationally excited. Its observation also testifies to the vibrational relaxation of the ^{3}MLCT excited state. On the other hand, the rise dynamics of the excited-state Raman bands is a very unusual effect which needs to be examined in more detail.

Measurement of antistokes TR^3 spectra of the ^{3}MLCT excited state was attempted using both pumping and probing at 400 nm at time delays of 1, 5, and 10 ps. The spectra do not show any excited-state bands. However, the presence of weak solvent and ground-state bands at low frequencies (up to ca. 950 cm^{-1}) indicate that that absence of excited-state bands is not an experimental artifact. It can thus be concluded that excitation of high-frequency, dmb-localized vibrational modes in the ^{3}MLCT state is decayed already at 1−5 ps after its population.

TR^3 spectra of [Re(Cl)$(CO)_3$(bpy)] show characteristic bands of the $bpy^{\bullet-}$ chromophore which rise in intensity during the first 20 ps; see Figure 5. The strong band at 1286 cm^{-1} and the weaker band at 1553 cm^{-1} are especially diagnostic for the Re → bpy ^{3}MLCT excited state, which can be formulated as [Re^{II}(Cl)$(CO)_3(bpy^{\bullet-})$]. These bands are well-separated from interfering ground-state and solvent bands. They are prominent also in the nanosecond transient resonance Raman spectra of both [Re(Cl)$(CO)_3$(bpy)] and $[Ru(bpy)_3]^{2+}$ and were attributed to mixed ν(CC) and ν(CN) vibrations of the $bpy^{\bullet-}$ ligand.[48,50,52,61,62] The vibration responsible for the 1286 cm^{-1} peak contains an important contribution from the $bpy^{\bullet-}$ inter-ring CC stretch.[52] The TR^3 band positions of [Re(Cl)$(CO)_3$(bpy)] do not show any systematic dynamical shifts above the experimental uncertainty.

Time-resolved UV−vis absorption spectra of [Re(Etpy)$(CO)_3$(dmb)]$^+$ show an intense, sharp band at 375 nm, followed by a weaker band at 455 nm, see Figure 6. The same bands occur in

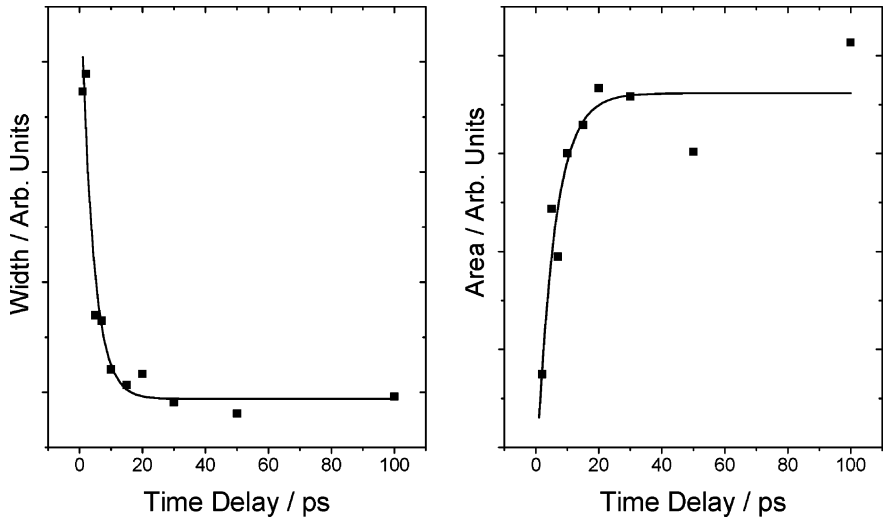

Figure 4. Raman dynamics observed in the TR^3 spectra of [Re(Etpy)$(CO)_3$(dmb)]$^+$ in CH_3CN after excitation with 400 nm, 1−2 ps laser pulses and probed with delayed 400 nm, 1−2 ps laser pulses. The long-lived emission was rejected using a 4 ps Kerr gate. Left: time-dependent width (fwhm) of the 1497 cm^{-1} band. Fitted to a single-exponential decay; 4 ± 1 ps. Right: time-dependent area of the 1195 cm^{-1} band. Fitted to a single-exponential rise; 6 ± 2 ps.

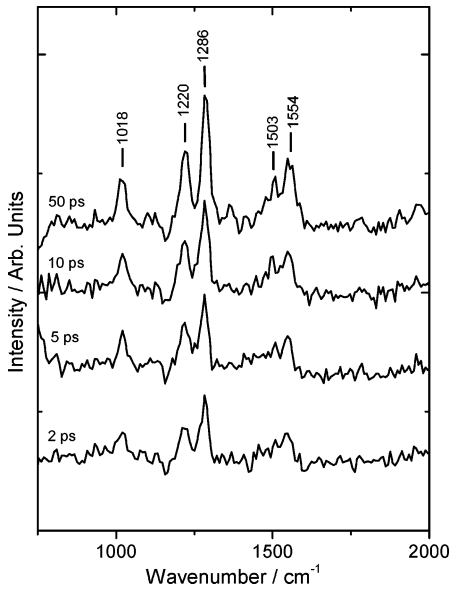

Figure 5. Picosecond time-resolved resonance Raman spectra of [Re(Cl)(CO)$_3$(bpy)] in CH_2Cl_2 measured at 2, 5, 10, and 50 ps after excitation with 400 nm, 1−2 ps laser pulses and probed with delayed 400 nm, 1−2 ps laser pulses. The long-lived emission was rejected using a 4 ps Kerr gate.

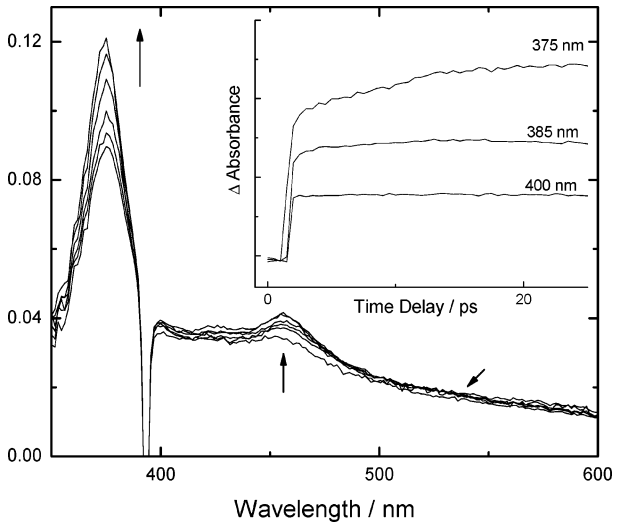

Figure 6. Difference time-resolved UV−vis absorption spectra of [Re(Etpy)(CO)$_3$(dmb)]$^+$ in CH_3CN. Spectra measured at 2.5, 3, 5 10, 15, and 40 ps after excitation with a 390 nm, ca. 130 fs laser pulse are shown in the direction of the arrows. The white-light continuum was optimized for the near-UV and the violet-blue regions of the spectrum. The sharp dip at 390 nm is caused by stray laser pump light. Inset: absorbance−time profiles measured at selected probe wavelengths.

the time-resolved spectra of [Re(Cl)(CO)$_3$(bpy)] at 378 and 475 nm. Hereafter, these features will be discussed together for both complexes and denoted 375/378 and 455/475 nm, respectively. Transient absorption spectra of both complexes also show a shoulder at ∼550 nm tailing to the red spectral region. All these spectral features originate in $\pi\pi^*$ transitions of the dmb$^{\bullet-}$ or bpy$^{\bullet-}$ ligands,[38,63−66] in accordance with the formulation of the ^{3}MLCT excited states as [Re^{II}(Etpy)(CO)$_3$(dmb$^{\bullet-}$)]$^+$ and [Re^{II}(Cl)(CO)$_3$(bpy$^{\bullet-}$)], respectively. Time-resolved UV−vis spectra of both [Re(Etpy)(CO)$_3$(dmb)]$^+$ and [Re(Cl)(CO)$_3$(bpy)] show a sharp, instrument-limited absorbance rise, followed by further dynamical evolution during the first ca. 20 ps, which depends on the probe wavelength, Figure 6. Absorption at wavelengths of 550 nm and longer slightly decreases during the first ca. 4 ps. In contrast, the 375/378 and 455/475 nm bands increase in intensity. This growth is more prominent for the 375/378 nm band whose maximum intensity increases by ca. 25% during the first ∼15 ps. It should be noted that the absorbance at the wavelength corresponding to the half-maximum of the 375/378 nm absorption band increases as well. On the other hand, the absorbance is essentially time-independent in the flat region between the 375/378 and 455/475 nm bands.

Discussion

The ground-state preresonance Raman spectrum demonstrates the Re → dmb ^{1}MLCT character of the lowest allowed electronic transition of [Re(Etpy)(CO)$_3$(dmb)]$^+$. Time-resolved emission and IR absorption spectra confirm the ^{3}MLCT character of the lowest-lying relaxed excited state, i.e., ^{3}[Re^{II}(Etpy)(CO)$_3$(dmb$^{\bullet-}$)]$^+$. In agreement with this formulation, excited-state UV−vis absorption and resonance Raman spectra show features due to the reduced dmb$^{\bullet-}$ ligand. Remarkably, excited-state Raman bands grow-in with a ∼6 ps rise time. The 375 and 455 nm dmb$^{\bullet-}$ absorption bands also increase in intensity during the first 15−20 ps. The rise in excited-state Raman and UV absorption band intensities is paralleled by a shift of ν(CO) IR bands and at least two of the dmb$^{\bullet-}$ Raman bands to higher wavenumbers, which occurs on a comparable or slightly longer time scale, with time constants up to ca. 11 ps. All IR and Raman bands narrow concomitantly. Dynamic changes in excited-state IR and Raman band positions and widths can be attributed[67−73] to vibrational cooling of low-frequency intramolecular, solute−solvent, and first solvation sphere vibrations that are anharmonically coupled to the high-frequency ν(CO) and dmb$^{\bullet-}$ modes. These low-frequency modes get highly excited during the femtosecond intersystem crossing from the ^{1}MLCT state, that is optically populated at 25 000 cm^{-1}, to the ^{3}MLCT state, for which a 0−0 energy of 18 700 cm^{-1} was determined.[55] Hence, ca. 6300 cm^{-1} excess energy has to be dissipated into vibrational modes on a femtosecond time scale. Vibrational relaxation (cooling) of the low-frequency modes then proceeds on a picosecond time scale by energy transfer to the surrounding solvent bath.[70] The picosecond growth of excited-state TR^3 and UV−vis bands is not restricted to [Re(Etpy)(CO)$_3$(bpy)]$^+$, as it was observed also for [Re(Cl)(CO)$_3$(bpy)].

While picosecond shifts and narrowing of Raman bands are rather common in TR^3 spectra of electronically excited organic molecules,[67−72] the rise in Raman intensities is a very rare phenomenon. As to our knowledge, it was, so far, described only for Raman spectra of aromatic cation-radicals generated by femtosecond 2-photon ionization in acetonitrile.[67] No such effect was observed for the same species in ethyl acetate. Raman bands were found to shift upward ∼15 cm^{-1} in both solvents with 13−17 ps time constants. The band-shift was explained by vibrational cooling while the intensity rise was attributed to *"thermal excitation of the neighboring solvent molecules that disturbs the solvation structure of the cation radical which causes the change in the value of its electronic transition moment"*.[67] However, time-resolved visible absorption spectra of the radical-cations were not presented. Moreover, it is not clear why the Raman rise dynamics of these radical-cations is so much solvent-dependent, while the vibrational cooling, manifested by the dynamic shift in Raman band positions, is not.[67]

Herein, we attribute the remarkable growth of excited-state Raman and visible absorption bands to vibrational cooling of low-frequency vibrations, which is clearly manifested by the dynamics in ν(CO) IR and dmb$^{\bullet-}$ Raman band positions and

widths. This conclusion is strongly supported by the fact that all these effects occur on comparable time-scales.

The rise of TR^3 band intensities is closely connected with the rise of the intensity of the resonant electronic transition, which occurs at 375 and 378 nm for $[Re(Etpy)(CO)_3(dmb)]^+$ and $[Re(Cl)(CO)_3(bpy)]$, respectively.[74] This is a $\pi\pi^*$ transition of the $NN^{\bullet-}$ ligand (NN = dmb, bpy), further denoted 1→2. Its transition moment is expressed as

$$\mu_{12} = -e\langle\psi_1|r|\psi_2\rangle\sum_{n_1,\upsilon_2}\langle n_1|\upsilon_2\rangle \qquad (1)$$

The (pre)resonance Raman intensity I_{n1m1} of a TR^3 band due to a $n_1 \rightarrow m_1$ vibrational transition in the electronic state 1 (= ^{3}MLCT) is described by the Albrecht A-term expression

$$I_{n1}m_1 \propto \mu_{el}^4\left[\sum_{n_1,\upsilon_2}\frac{\langle n_1|\upsilon_2\rangle\langle\upsilon_2|m_1\rangle}{\tilde{\nu}_{1m,2\upsilon} - \tilde{\nu}_0 + i\Gamma_{12}}\right]^2 \qquad (2)$$

Here, $\psi_{1,2}$, n_1, m_1, and υ_2 represent the electronic and vibrational wave functions of the electronic states 1 and 2, that is the ^{3}MLCT and the higher $\pi\pi^*(NN^{\bullet-})$ state, respectively. $\tilde{\nu}_{1m,2\upsilon}$ is the energy (in cm^{-1}) and μ_{el} the electronic transition moment $-e\langle\psi_1|r|\psi_2\rangle$ of the resonant electronic (vibronic) transition 1 → 2. $\tilde{\nu}_0$ is the Raman probe wavenumber. Γ_{12} stands for the damping factor. In the present case, we assume that the Raman enhancement originates predominantly in the $\pi\pi^*(NN^{\bullet-})$ transition at 375/378 nm, that is $\tilde{\nu}_{1m,2\upsilon}$= 26667/26455 cm^{-1}. The resonant electronic transition energy $\tilde{\nu}_{1m,2\upsilon}$ does not change with time as was manifested by the constant position of the 375/378 nm absorption band, Figure 6.

Equations 1 and 2 show that TR^3 and UV−vis band intensities are interrelated through both the electronic transition moment μ_{el} and vibrational overlap integrals $\langle n_1|\upsilon_2\rangle$. Vibrational cooling amounts to structural reorganization, which may affect shapes of the potential energy surfaces of the ^{3}MLCT and/or the upper $\pi\pi^*$ excited state. Vibrational overlap integrals $\langle n_1|\upsilon_2\rangle$, $\langle\upsilon_2|m_1\rangle$ and/or the electronic transition moment μ_{el} will then increase alongside vibrational cooling. This will be manifested by growth of both the 375/378 nm absorption band and resonantly enhanced Raman bands due to $NN^{\bullet-}$ intraligand vibrations.

This explanation relates well together the dynamical evolutions of excited-state Raman and UV−Vis band intensities with those of the IR and Raman band positions and widths. Nevertheless, alternative mechanisms need to be considered as well: (i) The initial ~6300 cm^{-1} excess of energy can be first deposited into high-frequency $NN^{\bullet-}$-localized modes. Picosecond rise of Stokes TR^3 band intensities would then correspond to intramolecular vibrational energy redistribution (IVR) from these vibrational levels ($n_1 \geq 1$) into the $n_1 = 0$ level, for which higher values of the vibrational overlap integral $\langle n_1|\upsilon_2\rangle$ can be expected. Intensities of both the transient UV−vis absorption and (pre)resonance Raman band would increase alongside. This explanation seems to be disproved by the absence of any excited-state bands in the antistokes TR^3 spectra of $[Re(Etpy)(CO)_3(dmb)]^+$, which would demonstrate the initial population on $n_1 \geq 1$ levels. (ii) ^{3}MLCT excited states on Re carbonyl-diimine actually occur as a manifold of three excited states with a very similar Re → NN ^{3}MLCT character. They originate in excitations from different Re d_π orbitals into the same NN-based π^* LUMO. Moreover, each of these ^{3}MLCT states is split into three spin−orbit sublevels. Intersystem crossing from the optically excited ^{1}MLCT state could be followed by equilibration of the ^{3}MLCT manifold, manifested by the observed picosecond dynamics. However, such an electronic relaxation of closely spaced excited-states is expected to occur on a femtosecond time scale, as was observed, e.g. for $[Ru(bpy)_3]^{2+}$ and its analogues.[26,27] Moreover, no evidence for such process was seen in ps TR^3 spectra of a similar carbonyl complex[W(4-cyanopyridine)$(CO)_5$], which also possesses a low-lying ^{3}MLCT manifold.[75]

Conclusions

^{3}MLCT excited states of $[Re(Etpy)(CO)_3(dmb)]^+$ and $[Re(Cl)(CO)_3(bpy)]$ are initially formed highly vibrationally excited in low-frequency modes which are anharmonically coupled to ν(CO) and $NN^{\bullet-}$ vibrations (NN = dmb, bpy). Vibrational relaxation (cooling) occurs with time constants in the range 1−11 ps, driving the excited molecule toward its equilibrated molecular and solvation structure. This is manifested by picosecond upward shifts of ν(CO) IR and $dmb^{\bullet-}$ Raman bands and by their narrowing. Remarkably, intensities of excited-state $\pi\pi^*(NN^{\bullet-})$ (pre)resonance Raman and UV−vis absorption bands increase on the same time scale. The growth of the UV−vis absorption and resonance Raman bands are interrelated. It is attributed to structural relaxation during vibrational cooling which modifies the shapes of relevant potential energy surfaces, increasing the electronic transition moment and/or vibrational overlap.

It can be reasonably expected that the same type of vibrational relaxation occurs in MLCT excited states of other complexes containing M(polypyridine) or M(α-diimine) chromophores. The observation that M → polypyridine ^{3}MLCT excited states remain vibrationally hot on a picosecond time scale implies that ultrafast photochemical processes of metal polypyridine complexes actually occur from unequilibrated, vibrationally hot states. This applies, for example, to important processes of electron injection into semiconductors, inter-ligand electron transfer, or intramolecular charge separation.

Acknowledgment. Femtosecond near-UV time-resolved absorption spectra were measured with the kind help of Mr. M. Groeneveld at the Institute of Molecular Chemistry, University of Amsterdam. Financial support from EPSRC and COST D14 Action is gratefully appreciated.

References and Notes

(1) Juris, A.; Balzani, V.; Barigelletti, F.; Campagna, S.; Belser, P.; von Zelewsky, A. *Coord. Chem. Rev.* **1988**, *84*, 85.

(2) Geoffroy, G. L.; Wrighton, M. S. *Organometallic Photochemistry*; Academic Press: New York, 1979.

(3) Stufkens, D. J. *Comments Inorg. Chem.* **1992**, *13*, 359.

(4) Vlček, A., Jr. In *Electron Transfer in Chemistry*; Balzani, V., Astruc, D., Eds.; Wiley-VCH: Weinheim, 2001; Vol. 2, p 804.

(5) Tachibana, Y.; Moser, J. E.; Grätzel, M.; Klug, D. R.; Durrant, J. R. *J. Phys. Chem.* **1996**, *100*, 20056.

(6) Benkö, G.; Kallioinen, J.; Korppi-Tommola, J. E. I.; Yartsev, A. P.; Sundström, V. *J. Am. Chem. Soc.* **2002**, *124*, 489.

(7) Kallioinen, J.; Benkö, G.; Sundström, V.; Korppi-Tommola, J. E. I.; Yartsev, A. P. *J. Phys. Phem. B* **2002**, *106*, 4396.

(8) Asbury, J. B.; Ellingson, R. J.; Ghosh, H. N.; Ferrere, S.; Nozik, A. J.; Lian, T. *J. Phys. Chem. B* **1999**, *103*, 3110.

(9) Ellingson, R. J.; Asbury, J. B.; Ferrere, S.; Ghosh, H. N.; Sprague, J. R.; Lian, T.; Nozik, A. J. *J. Phys. Chem. B* **1998**, *102*, 6455.

(10) Asbury, J. B.; Hao, E.; Wang, Y.; Ghosh, H. N.; Lian, T. *J. Phys. Chem. B* **2001**, *105*, 4545.

(11) Wang, Y.; Asbury, J. B.; Lian, T. *J. Phys. Chem. A* **2000**, *104*, 4291.

(12) Chen, P.; Mecklenburg, S. L.; Meyer, T. J. *J. Phys. Chem.* **1993**, *97*, 13126.

(13) Liard, D. J.; Vlček, A., Jr. *Inorg. Chem.* **2000**, *39*, 485.

(14) Liard, D. J.; Busby, M.; Farrell, I. R.; Matousek, P.; Towrie, M.; Vlček, A., Jr. *J. Phys. Chem. A* **2004**, *108*, 556.

(15) Wang, Y.; Hauser, B. T.; Rooney, M. M.; Burton, R. D.; Schanze, K. S. *J. Am. Chem. Soc.* **1993**, *115*, 5675.
(16) Chen, P.; Westmoreland, T. D.; Danielson, E.; Schanze, K. S.; Anthon, D.; Neveux, P. E., Jr.; Meyer, T. J. *Inorg. Chem.* **1987**, *26*, 1116.
(17) Chen, P.; Duesing, R.; Graff, D. K.; Meyer, T. J. *J. Phys. Chem.* **1991**, *95*, 5850.
(18) Trammell, S.; Goodson, P. A.; Sullivan, B. P. *Inorg. Chem.* **1996**, *35*, 1421.
(19) Chen, P.; Danielson, E.; Meyer, T. J. *J. Phys. Chem.* **1988**, *92*, 3708.
(20) Schoonover, J. R.; Chen, P.; Bates, W. D.; Dyer, R. B.; Meyer, T. J. *Inorg. Chem.* **1994**, *33*, 793.
(21) Schoonover, J. R.; Strouse, G. F.; Chen, P.; Bates, W. D.; Meyer, T. J. *Inorg. Chem.* **1993**, *32*, 2618.
(22) Cabana, L. A.; Schanze, K. S. *Adv. Chem. Ser.* **1990**, *226*, 101.
(23) Lucia, L. A.; Wang, Y.; Nafisi, K.; Netzel, T. L.; Schanze, K. S. *J. Phys. Chem.* **1995**, *99*, 11801.
(24) Wang, Y.; Lucia, L. A.; Schanze, K. S. *J. Phys. Chem.* **1995**, *99*, 1961.
(25) Wang, Y.; Schanze, K. S. *J. Phys. Chem.* **1996**, *100*, 5408.
(26) Damrauer, N. H.; Cerullo, G.; Yeh, A.; Boussie, T. R.; Shank, C. V.; McCusker, J. K. *Science* **1997**, *275*, 54.
(27) Yeh, A. T.; Shank, C. V.; McCusker, J. K. *Science* **2000**, *289*, 935.
(28) Bhasikuttan, A. C.; Suzuki, M.; Nakashima, S.; Okada, T. *J. Am. Chem. Soc.* **2002**, *124*, 8398.
(29) Damrauer, N. H.; McCusker, J. K. *J. Phys. Chem. A* **1999**, *103*, 8440.
(30) Huber, R.; Moser, J.-E.; Grätzel, M.; Wachtveitl, J. *J. Phys. Chem. B* **2002**, *106*, 6494.
(31) Önfelt, B.; Lincoln, P.; Nordén, B.; Baskin, J. S.; Zewail, A. H. *Proc. Natl. Acad. Sci. U.S.A.* **2000**, *97*, 5708.
(32) Shaw, G. B.; Brown, C. L.; Papanikolas, J. M. *J. Phys. Chem. A* **2002**, *106*, 1483.
(33) Asbury, J. B.; Wang, Y.; Lian, T. *Bull. Chem. Soc. Jpn.* **2002**, *75*, 973.
(34) Worl, L. A.; Duesing, R.; Chen, P.; Della Ciana, L.; Meyer, T. J. *J. Chem. Soc., Dalton Trans.* **1991**, 849.
(35) Stufkens, D. J.; Vlček, A., Jr. *Coord. Chem. Rev.* **1998**, *177*, 127.
(36) Wrighton, M. S.; Morse, D. L. *J. Am. Chem. Soc.* **1974**, *96*, 998.
(37) Luong, J. C.; Nadjo, L.; Wrighton, M. S. *J. Am. Chem. Soc.* **1978**, *100*, 5790.
(38) Kalyanasundaram, K. *J. Chem. Soc., Faraday Trans. 2* **1986**, *82*, 2401.
(39) Busby, M.; Liard, D. J.; Motevalli, M.; Toms, H.; Vlček, A., Jr. *Inorg. Chim. Acta* **2004**, *357*, 167.
(40) Staal, L. H.; Oskam, A.; Vrieze, K. *J. Organomet. Chem.* **1979**, *170*, 235.
(41) Vlček, A., Jr.; Farrell, I. R.; Liard, D. J.; Matousek, P.; Towrie, M.; Parker, A. W.; Grills, D. C.; George, M. W. *J. Chem. Soc., Dalton Trans.* **2002**, 701.
(42) Matousek, P.; Parker, A. W.; Taday, P. F.; Toner, W. T.; Towrie, M. *Opt. Comm.* **1996**, *127*, 307.
(43) Towrie, M.; Parker, A. W.; Shaikh, W.; Matousek, P. *Meas. Sci. Technol.* **1998**, *9*, 816.
(44) Matousek, P.; Towrie, M.; Stanley, A.; Parker, A. W. *Appl. Spectrosc.* **1999**, *53*, 1485.
(45) Matousek, P.; Towrie, M.; Ma, C.; Kwok, W. M.; Phillips, D.; Toner, W. T.; Parker, A. W. *J. Raman Spectrosc.* **2001**, *32*, 983.
(46) Towrie, M.; Grills, D. C.; Dyer, J.; Weinstein, J. A.; Matousek, P.; Barton, R.; Bailey, P. D.; Subramaniam, N.; Kwok, W. M.; Ma, C. S.; Phillips, D.; Parker, A. W.; George, M. W. *Appl. Spectrosc.* **2003**, *57*, 367.
(47) Vergeer, F. W.; Kleverlaan, C. J.; Stufkens, D. J. *Inorg. Chim. Acta* **2002**, *327*, 126.
(48) Treffert-Ziemelis, S. M.; Golus, J.; Strommen, D. P.; Kincaid, J. R. *Inorg. Chem.* **1993**, *32*, 3890.
(49) Vlček, A. J. *Coord. Chem. Rev.* **2002**, *230*, 225.
(50) Smothers, W. K.; Wrighton, M. S. *J. Am. Chem. Soc.* **1983**, *105*, 1067.
(51) Mallick, P. K.; Strommen, D. P.; Kincaid, J. R. *J. Am. Chem. Soc.* **1990**, *112*, 1686.
(52) Mallick, P. K.; Danzer, G. D.; Strommen, D. P.; Kincaid, J. R. *J. Phys. Chem.* **1988**, *92*, 5628.
(53) Záliš, S.; Farrell, I. R.; Vlček, A., Jr. *J. Am. Chem. Soc.* **2003**, *125*, 4580.
(54) Claude, J. P.; Omberg, K. M.; Williams, D. S.; Meyer, T. J. *J. Phys. Chem. A* **2002**, *106*, 7795.
(55) Dattelbaum, D. M.; Omberg, K. M.; Schoonover, J. R.; Martin, R. L.; Meyer, T. J. *Inorg. Chem.* **2002**, *41*, 6071.
(56) Gamelin, D. R.; George, M. W.; Glyn, P.; Grevels, F.-W.; Johnson, F. P. A.; Klotzbucher, W.; Morrison, S. L.; Russell, G.; Schaffner, K.; Turner, J. J. *Inorg. Chem.* **1994**, *33*, 3246.
(57) George, M. W.; Johnson, F. P. A.; Westwell, J. R.; Hodges, P. M.; Turner, J. J. *J. Chem. Soc., Dalton Trans.* **1993**, 2977.
(58) Turner, J. J. *Coord. Chem. Rev.* **2002**, *230*, 212.
(59) The magnitudes of dynamical band shifts are extrapolated to time zero. The following dynamics were estimated for the other two excited-state ν(CO) bands: A′(2) band at 2013 cm^{-1}: shift $+15.5 \pm 3$ cm^{-1}; $\tau = 1 \pm 0.4$ ps (68%), 7.2 ± 1.8 ps (32%). A″ band at 1970 cm^{-1}: shift ca. $+3.1$ cm^{-1} 3.7 ± 0.3 ps. These values are less accurate than those determined for the A′(1) band (see the text) because of the overlap with the negative bleach bands. The small initial increase (deepening) of the 1930 cm^{-1} bleach is caused by narrowing and upward shift of the A″ band, which seems to occur initially at much lower wavenumbers than indicated by the Lorentzian analysis.
(60) Rosenthal, S. J.; Xie, X.; Du, M.; Fleming, G. R. *J. Chem. Phys.* **1991**, *95*, 4715.
(61) Woodruff, W. H.; Dallinger, R. F. *J. Am. Chem. Soc.* **1979**, *101*, 4391.
(62) Forster, M.; Hester, R. E. *Chem. Phys. Lett.* **1981**, *81*, 42.
(63) Noble, B. C.; Peacock, R. D. *Spectrochim. Acta* **1990**, *46A*, 407.
(64) Braterman, P. S.; Song, J.-I. *J. Org. Chem.* **1991**, *56*, 4678.
(65) König, E.; Kremer, S. *Chem. Phys. Lett.* **1970**, *5*, 87.
(66) Krejčik, M.; Vlček, A. A. *J. Electroanal. Chem.* **1991**, *313*, 243.
(67) Nakabayashi, T.; Kamo, S.; Sakuragi, H.; Nishi, N. *J. Phys. Chem. A* **2001**, *105*, 8605.
(68) Leonard, J. D., Jr.; Gustafson, T. L. *J. Phys. Chem. A* **2001**, *105*, 1724.
(69) Hamaguchi, H.; Iwata, K. *Bull. Chem. Soc. Jpn.* **2002**, *75*, 883.
(70) Iwata, K.; Hamaguchi, H. *J. Phys. Chem. A* **1997**, *101*, 632.
(71) Werncke, W.; Wachsmann-Hogiu, S.; Dreyer, J.; Vodchits, A. I.; Elsaesser, T. *Bull. Chem. Soc. Jpn.* **2002**, *75*, 1049.
(72) Scholes, G. D.; Matousek, P.; Parker, A. W.; Phillips, D.; Towrie, M. *J. Phys. Chem. A* **1998**, *102*, 1431.
(73) Lian, T.; Bromberg, S. E.; Asplund, M. C.; Yang, H.; Harris, C. B. *J. Phys. Chem.* **1996**, *100*, 11994.
(74) The possibility that the early excited-state evolution of the TR^3 and TA spectra is due to increasing population of the ^{3}MLCT state or time-dependent reabsorption of the Raman-scattered light can be excluded on the following grounds: (i) The increase of UV−vis excited-state absorption occurs only at certain wavelengths whereas a uniform increase is expected to manifest population dynamics. Integrated areas of excited-state IR bands are time-independent. (ii) Raman scattering occurs in the plateau of the transient absorption spectrum, between 410 and 430 nm, where the absorbance hardly changes with time, Figure 6.
(75) Záliš, S.; Busby, M.; Kotrba, T.; Matousek, P.; Towrie, M.; Vlček, A., Jr. *Inorg. Chem.* **2004** *43*, 1723.